analytical chemistry

Letter

pubs.acs.org/ac

A 3D Printed Fluidic Device that Enables Integrated Features

Kari B. Anderson,[†] Sarah Y. Lockwood,[†] R. Scott Martin,[§] and Dana M. Spence*,[†]

[†]Department of Chemistry, Michigan State University, East Lansing, Michigan 48824, United States

[§]Department of Chemistry, Saint Louis University, St. Louis, Missouri 63103, United States

ABSTRACT: Fluidic devices fabricated using conventional soft lithography are well suited as prototyping methods. Three-dimensional (3D) printing, commonly used for producing design prototypes in industry, allows for one step production of devices. 3D printers build a device layer by layer based on 3D computer models. Here, a reusable, high throughput, 3D printed fluidic device was created that enables flow and incorporates a membrane above a channel in order to study drug transport and affect cells. The device contains 8 parallel channels, 3 mm wide by 1.5 mm deep, connected to a syringe pump through standard, threaded fittings. The device was also printed to allow integration with commercially available membrane inserts whose bottoms are constructed of a porous polycarbonate membrane; this insert enables molecular transport to occur from the channel to above the well. When concentrations of various antibiotics (levofloxacin and linezolid) are pumped through the channels, approximately 18−21% of the drug migrates through the porous membrane, providing evidence that this device will be useful for studies where drug effects on cells are investigated. Finally, we show that mammalian cells cultured on this membrane can be affected by reagents flowing through the channels. Specifically, saponin was used to compromise cell membranes, and a fluorescent label was used to monitor the extent, resulting in a 4-fold increase in fluorescence for saponin treated cells.

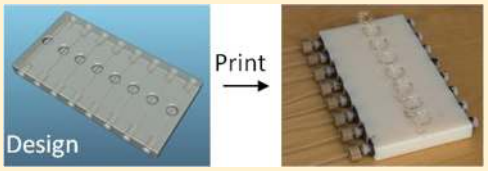

The microfluidic devices utilized for assays in most academic laboratories are generally prepared using methods suited for rapid prototyping, such as conventional and soft lithography.[1,2] Recently, efforts have been made to produce devices that combine soft lithographic methods with embossing techniques. Work from Albritton, Beebe, and our own laboratories have produced prototypes from polystyrene that are rugged and robust but also simple to fabricate with conventional soft lithographic techniques.[3−6] Here, we report that three-dimensional (3D) printing enables essentially a one-step rapid production of devices that are rugged, robust, and reusable.

3D printing has commonly been used in manufacturing industries to produce design prototypes, but recently, it has been utilized in the areas of scaffolds for tissue growth,[7−10] prototyping,[11,12] electronics,[13] microfluidics,[14,15] and pneumatics.[16] 3D printers build a device, layer by layer, based on "sliced" 3D models that are drawn using a computer program, such as Computer Aided Design (CAD).[17,18] An advantage of 3D printed devices is that they can be printed on demand, and the design files could be shared online or as part of the publication process so that technology can be shared between laboratories in a reproducible manner. Here, a fluidic device is created using a 3D printer that constructs the device layer by layer by inkjet deposition of photopolymerizable materials that are hardened by subsequent UV irradiation. The printer is able to print polymer droplets that are 42 μm in diameter, which allows for features as small as 100 μm.

Previously, fluidic devices that enable mixing[14] and chambers for organic reactions[15] have been fabricated, as well as scaffolds allowing for cell growth.[9] However, to date, no device has been directly printed that incorporates flow of a sample for subsequent detection of analytes of interest in that sample. Furthermore, 3D printed devices will greatly enhance device modularity and ease of use by using printed threads for fluidic connectors. We will also demonstrate our ability to measure drug transport across a membrane and affect cells cultured on the membrane-based insert that is placed into the device after it is printed.

MATERIALS AND METHODS

3D Printed Device Fabrication. All 3D printed devices were printed on an Objet Connex 350 printer housed in the Department of Electrical and Computer Engineering at Michigan State University. Device designs were created using either McNeel Rhinoceros or PTC Creo software. All devices were printed using Objet Vero White Plus material whose exact composition is proprietary but approximately contains: isobornyl acrylate (15−30%), acrylic monomer (15−30%), urethane acrylate (15−50%), epoxy acrylate (5−10; 10−15%), acrylic monomer (5−10; 10−15%), acrylic oligomer (5−10; 10−15%), and photoinitiator (0.1−1; 1−2%). Once printed, the devices are opaque, white, and rigid. Initial prototypes contained only one channel, but as many as 8 channels on one device have been successfully printed. Using commercially available cell culture inserts (0.4 μm pore diameter, Corning Incorporated, Corning, NY, USA), polycarbonate membranes were clicked into a 9 mm port placed above the channel. The channels are 3.0 mm wide and 1.5 mm deep under the membrane. To integrate the devices with syringes for pumping,

Received: April 1, 2013
Accepted: May 21, 2013
Published: May 21, 2013

   dx.doi.org/10.1021/ac4009594 | *Anal. Chem.* 2013, 85, 5622−5626

the inlet was printed so that a female luer adapter (P-629, IDEX Health and Science, Oak Harbor, WA, USA) could be clicked into place and sealed with quick drying epoxy. In this manner, syringes were connected to the device via this adapter and a dual syringe pump was used to propel sample through the channels. All of the experiments were performed at room temperature, approximately 22 °C.

Sample Preparation for Drug Transport. To study drug transport in the 3D printed device, two established drugs, levofloxacin (Sigma Aldrich, St. Louis, MO, USA) and linezolid (TOCRIS Bioscience, Bristol, United Kingdom), were prepared in standard solutions ranging from 100 to 2000 nM in physiological salt solution (PSS) composed of 2.0 mM $CaCl_2$, 4.7 mM KCl, 11.1 mM dextrose, 12 mM $MgSO_4$, 21.0 mM tris(hydroxymethyl)aminomethane, and 140.5 mM NaCl (final pH 7.4) (Sigma Aldrich, St. Louis, MO, USA) as a buffer. Standards were then pumped at 1 μL/min through the channels of the 3D device for 1 h. In this case, the cell culture inserts that were clicked in above the channel contained 150 μL of PSS, and from that, aliquots of sample (25 μL) were taken after an hour of pumping. The 25 μL samples were added to 96 μL of cold acetonitrile (Mallinckrodt Chemicals, Phillipsburg, NJ, USA) containing the internal standard, 750 nM ciprofloxacin (Sigma Aldrich, St Louis, MO). To remove any precipitants, samples were centrifuged (500*g* for 10 min) and the supernatant was removed. After centrifugation, the samples were added to a 96-well polycarbonate plate (Denville, Metuchen, NJ, USA) and sealed using a RapidEPS seal (Bio Chromato, Fujisawa, Japan).

Mass Spectrometric Analysis of Drug Transport. Detection of the drugs was achieved by using a Shimadzu high performance liquid chromatograph (HPLC) coupled with multiple reaction tandem monitoring mass spectrometry (MRM-MS/MS) with electrospray ionization (ESI) using a Waters Quattro Micro triple quadrupole mass spectrometer. The reverse phase HPLC separation was performed through the use of a Supelco Ascentis precolumn, followed by a packed Supelco Ascentis Express C18 column (length: 3 cm; ID: 2.1 mm; particles: 2.7 μm) (Supelco, Bellefonte, PA, USA). A 10 μL sample from the 96-well plate was injected onto the column where it underwent separation at 0.45 mL/min with the corresponding gradient, 95% A, 0% B for 0.25 min; 2% A, 0% B at 1.00 min; 2% A, 0% B at 1.25 min; 30% A, 15% B at 1.75 min; 30% A, 15% B at 1.90 min; 95% A, 0% B at 2.00 min. Solvent A is methanol; solvent B is acetonitrile, and solvent C is 1% formic acid in water. Retention times of ciprofloxacin, levofloxacin, and linezolid are 1.51, 1.48, and 1.71 min, respectively.

Upon introduction into the Quattro Micro mass spectrometer, analytes were ionized by ESI and further analyzed using the MRM-MS/MS. Cone voltages were 25 and 30 V for ciprofloxacin and levofloxacin/linezolid, respectively. Collision energies for ciprofloxacin, levofloxacin, and linezolid were 40, 30, and 35 eV, respectively. The MRM transitions monitored were 332.11 > 231.06 (ciprofloxacin), 362.11 > 234.05 (levofloxacin), and 338.13 > 296.1 m/z (linezolid). The collision gas, argon, was 1.96×10^{-3} Torr. Quantitative data processing was obtained through Waters MassLynx software (Milford, MA, USA). Calibration curves were generated by taking the ratio of sample peak area to the internal standard peak area.

Endothelial Cell Culture onto Inserts. Bovine pulmonary artery endothelial cells (ECs) were used in all cell studies. Cell culture on the inserts was performed similar to previous methods.[19] Immediately prior to culturing cells on the insert, cells were stained with Hoechst 33342 dye (Invitrogen, Grand Island, NY, USA). The Hoechst dye stains nuclei so that cells can be visualized using fluorescence microscopy.

Hoechst dye stained ECs were then seeded onto 6.5 mm membrane inserts that contain a permeable polycarbonate membrane (0.4 μm pore diameter, Corning Incorporated, Corning, NY, USA). The cells were allowed to grow to confluence for 24 h as visualized by optical microscopy. Membrane inserts were then clicked into place above the channels on the 3D printed device, and 100 μL of Hank's balanced salt solution (HBSS, Sigma Aldrich, St. Louis, MO, USA) was pipetted onto the insert.

Sample Preparation and Experimental Procedure for Cell Viability Study. Saponin (Sigma Aldrich, St. Louis, MO, USA), a known cell detergent, was used to permeabilize EC membranes in order to induce death. Saponin (0.025% in HBSS), or HBSS, was then loaded into syringes and flowed through the 3D printed device underneath the membrane insert containing cultured ECs, for 30 min at 1 μL/min using a dual syringe pump. The inserts were then removed from the device and placed into a 24 well plate containing 600 μL of HBSS in the lower chamber.

The nucleic acid stain Sytox Green (Invitrogen, Grand Island, NY, USA), which only labels cells with compromised membranes, was used to determine whether or not saponin had killed the ECs. Its excitation and emission maxima are 504 and 523 nm, respectively, when bound to DNA. After saponin or HBSS was flowed under the cells, 4 μL of 1 μM Sytox Green was added to the membrane insert, resulting in a concentration of 40 nM above the cells. The probe was allowed to incubate at 37 °C for 30 min and then imaged using fluorescence microscopy. An Olympus MVX10 macroscope (Olympus America, Melville, NY, USA) was used to collect fluorescence images for each insert, and using the MicroSuite Biological Suite software (Olympus America, Melville, NY, USA), average pixel intensities of the fluorescence image were obtained. The data corresponding to the saponin treated cell insert was normalized to the data from the control cell insert with HBSS flowing through the channel. All images were taken after removing the insert from the device and placing it into a 24 well plate. It should be noted that images can also be taken with the inserts in place on the device.

RESULTS AND DISCUSSION

The device design used in these studies consisted of 8 channels with inlets allowing for sample introduction/syringe pump integration, analytical wells for membrane containing cell culture inserts, and outlets for waste. The design was created in McNeel Rhinoceros or PTC Creo software and took approximately 4 h to print. A printed device ready for analysis is shown in Figure 1. The side profile of one channel (Figure 1) shows how each channel will address the membrane allowing for diffusion of analytes from the channel, through the membrane, to the area above the insert. This device was used to study drug transport across the membrane.

Drug Transport across a Membrane. Standard samples containing linezolid and levofloxacin were prepared in PSS buffer. Concentrations of 1.1 and 2.0 μM standard solutions were introduced to the 3D device through syringes and soft Teflon tubing. The 3D device included a 3 mm channel directly under an open well that was fitted to the membrane insert.

dx.doi.org/10.1021/ac4009594 | *Anal. Chem.* 2013, 85, 5622−5626

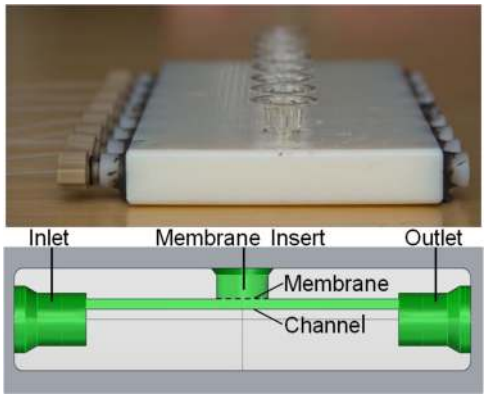

Figure 1. 3D printed device design. The final 3D printed device, top image, contains adapters for syringe-based pumps, channels, membrane insertion port, and outlets. The side view schematic of the device shows how the inlet addresses the channel and allows fluid to flow under the membrane. The membrane is part of a commercially available membrane insert that is manually inserted into the port on top of the device. Finally, there is an outlet to allow fluid to leave the device.

Upon insertion of the membrane insert, buffer was added to the insert and the standard solutions were pumped through the channels for an hour at 1 μL/min. After an hour, liquid was sampled from the insert and added to a vial containing a solution of acetonitrile and the internal standard, ciprofloxacin.

The samples were then analyzed using LC/MS/MS to monitor the diffusion of linezolid and levofloxacin from the channel, across the porous membrane. After an hour of flow, the 1.1 and 2 μM samples had between 18.4% and 20.5% drug transport across the polycarbonate membrane (Figure 2).

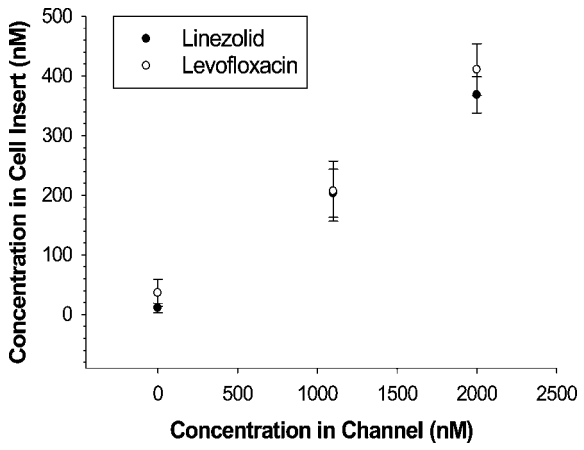

Figure 2. Drug transport across a membrane. Standards of the drugs linezolid (N = 4) and levofloxacin (N = 5) were flowed through the channels of the device; samples were collected above the membrane and analyzed via LC/MS/MS. As concentration of the drug increased, so did transport across the membrane with each concentration being statistically different from the previous (p value <0.001). Drug transport across the membrane was between 18.4% and 20.5%.

Moreover, results yielded reproducible drug transport concentrations between runs furthering the reusability of the device. Though it was not monitored in this instance, results from our lab indicate that drug transport can occur from the insert into the channel; of course, this transport is dependent upon the concentrations of the drug in the well and in the channel. If the concentration is higher in the channel, drug moves to the well; if higher in the well (e.g., if a gradient is performed that lowers the concentration in the channel), then the drug transport is back to the channel. Importantly, every molecule that we have tested to date has similar transport properties, with some differences occurring due to size of the molecule or its hydrophobicity.

In other polymer-based devices, reusability is not an option due to issues with maintaining seals. Contamination is also a concern due to challenges in cleaning devices or absorption of materials into the polymer base.[20] The use of a new device for each experiment can lead to high variability between runs. Also, the incorporation of a membrane into the polymer-based device, typically reversibly sealed between two pieces, can be easily compromised due to the flexibility of the support material. Cleaning and extended use can also weaken the fragile membrane. Many of these problems are minimized with the printed devices with well inserts.

Cell Viability Assessment. Commercially available cell culture inserts were used to integrate the 3D printed device with cultured cells. In this design, the insert clicks into place above the channel and the membrane would contain a layer of cultured cells as shown in Figure 3A. Furthermore, the ECs were stained with Hoechst 33342 dye (ex. 350 nm, em. 460 nm), a simple nucleic acid stain to confirm the presence of a confluent layer of cells on top of the membrane. The image in Figure 3A was obtained using a fluorescence microscope with a DAPI filter, and the stained cells are visualized on top of the membrane.

In order to determine whether this 3D printed device could be used to study cellular status, a viability study was performed using a well-known cell detergent and an EC line that is easily cultured onto membrane inserts. Either HBSS or saponin (a detergent used to compromise cell membranes) was flowed through the channel under the membrane that contained cultured ECs. It was expected that saponin would diffuse through the polycarbonate membrane and come into contact with the ECs. As shown in Figure 3B, the ECs that were treated with saponin had a 4-fold increase in fluorescence intensity in comparison to the cells treated with HBSS. The Sytox Green does not stain live cells, so the increased fluorescence indicates a higher population of dead cells. The images from the fluorescence microscope (Figure 3C) confirm this fact, as the image of the saponin treated ECs show more fluorescence than the image of ECs treated with HBSS alone.

The aforementioned strains on conventional fluidic membranes lend virtue to the cell culture insert as it has a rugged base, which supports the membrane and can be easily discarded after use. The rigidity of the 3D device when used simultaneously with the disposable cell inserts offers a supportive platform for a reusable fluidic device. Of course, many of these same features are available when using static 96-well plate systems. However, in a static system, the user is limited to adding a fixed amount of a drug candidate to cells cultured in a well on a microtiter plate and allowing that fixed amount of drug to interact with the cells for a predetermined amount of time before removing the drug from the cells in preparation for further dosing. The advantage of the 3D printed device described here is that each well/insert can be addressed by a fluidic stream. In this construct, the system now has the potential to function as a dynamic in vitro system; for example, the cells could be subjected to a drug candidate at a desirable concentration. However, by using gradient pumping schemes,

dx.doi.org/10.1021/ac4009594 | Anal. Chem. 2013, 85, 5622−5626

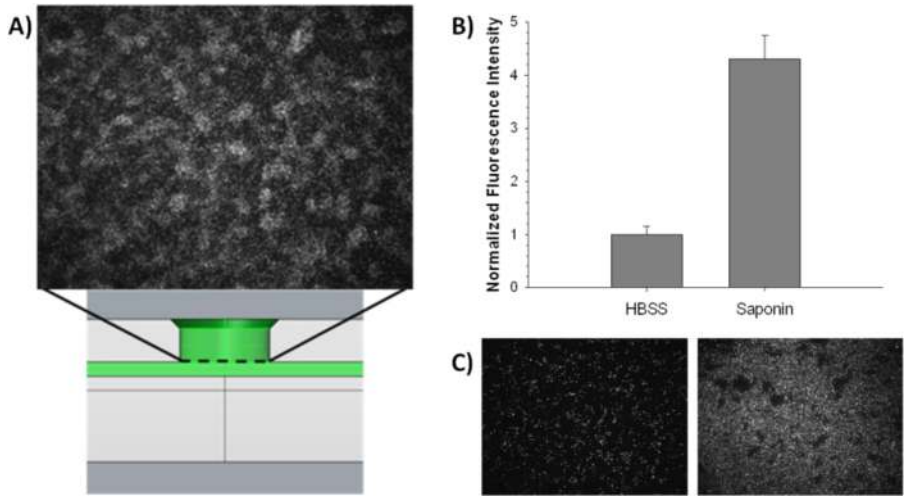

Figure 3. Incorporation of endothelial cells on 3D printed device and cell viability assessment. Endothelial cells were incorporated onto the 3D printed device by culturing them onto the membrane insert. (A) Cells were labeled with Hoechst 33342 dye, a nucleic acid stain, to confirm their presence on the membrane as evidenced in the fluorescent image. (B) Sytox Green was used to fluorescently label cells with compromised membranes. A 4-fold increase in Sytox Green fluorescence was observed in cells treated with saponin diffusing from the channel as compared to HBSS alone. (C) Fluorescence images representing cells treated with HBSS (left) and cells treated with saponin (right) incubated with Sytox Green.

the concentration being delivered to the cells could be decreased and drug would then transport from the well back to the channel. Depending on the slope of the gradient, the cells could be subjected to drug candidates, agonists, etc., with varying half-lives, minimum effective concentrations, and dosing regimens without manually removing the drug from the cells, a necessity of a static system.

CONCLUSIONS

The 3D printed device was capable of studying drug transport and cell viability in a parallel manner. This device design was intended for these specific academic studies, but there is great potential for utilizing 3D printed devices for highly automated and standard applications in industry. For example, because of the device ruggedness, standard fittings can be employed, which gives it an advantage over devices fabricated from soft polymers. Furthermore, the device shown in Figure 1 (with 8 channels) could easily be optimized for use in standard, high-throughput fluidic handling systems and plate readers. Additionally, the ability to rapidly modify and print prototypes is advantageous when optimizing a device design, and the possibility of design file sharing between laboratories would be beneficial. There are 17 different materials offered by Objet for their Connex printer, including a biocompatible material with medical approval; thus, optimization for experiments can also be performed using various combinations of these materials.

AUTHOR INFORMATION

Corresponding Author

*E-mail: dspence@chemistry.msu.edu. Phone: 517.355.9715 x174.

Notes

The authors declare no competing financial interest.

ACKNOWLEDGMENTS

The authors would like to thank Brian Wright in the Department of Electrical and Computer Engineering at Michigan State University for his help in 3D printing these devices, as well as Tekna design firm in Kalamazoo, MI, for their assistance in creating the necessary 3D .stl files. Furthermore, the authors would like to thank the Michigan State University RTSF Mass Spectrometry Core for assistance in instrumentation usage.

REFERENCES

(1) Duffy, D. C.; McDonald, J. C.; Schueller, O. J. A.; Whitesides, G. M. *Anal. Chem.* **1998**, *70*, 4974−4984.
(2) McDonald, J. C.; Duffy, D. C.; Anderson, J. R.; Chiu, D. T.; Wu, H.; Schueller, O. J. A.; Whitesides, G. M. *Electrophoresis* **2000**, *21*, 27−40.
(3) Young, E. W. K.; Berthier, E.; Guckenberger, D. J.; Sackmann, E.; Lamers, C.; Meyvantsson, I.; Huttenlocher, A.; Beebe, D. J. *Anal. Chem. (Washington, DC, U. S.)* **2011**, *83*, 1408−1417.
(4) Wang, Y.; Balowski, J.; Phillips, C.; Phillips, R.; Sims, C. E.; Allbritton, N. L. *Lab Chip* **2011**, *11*, 3089−3097.
(5) Anderson, K. B.; Halpin, S. T.; Johnson, A. S.; Martin, R. S.; Spence, D. M. *Analyst (Cambridge, United Kingdom)* **2013**, *138*, 137−143.
(6) Johnson, A. S.; Anderson, K. B.; Halpin, S. T.; Kirkpatrick, D. C.; Spence, D. M.; Martin, R. S. *Analyst (Cambridge, United Kingdom)* **2013**, *138*, 129−136.
(7) Shepherd, J. N. H.; Parker, S. T.; Shepherd, R. F.; Gillette, M. U.; Lewis, J. A.; Nuzzo, R. G. *Adv. Funct. Mater.* **2011**, *21*, 47−54.
(8) Lee, Y. B.; Polio, S.; Lee, W.; Dai, G. H.; Menon, L.; Carroll, R. S.; Yoo, S. S. *Exp. Neurol.* **2010**, *223*, 645−652.
(9) Lee, W.; Lee, V.; Polio, S.; Keegan, P.; Lee, J. H.; Fischer, K.; Park, J. K.; Yoo, S. S. *Biotechnol. Bioeng.* **2010**, *105*, 1178−1186.
(10) Butscher, A.; Bohner, M.; Hofmann, S.; Gauckler, L.; Muller, R. *Acta Biomater.* **2011**, *7*, 907−920.
(11) Stampfl, J.; Liska, R. *Macromol. Chem. Phys.* **2005**, *206*, 1253−1256.
(12) Rangel, D. P.; Superak, C.; Bielschowsky, M.; Farris, K.; Falconer, R. E.; Baveye, P. C. *Soil Sci. Soc. Am. J.* **2012**, *77*, 54−59.
(13) Ahn, B. Y.; Duoss, E. B.; Motala, M. J.; Guo, X. Y.; Park, S. I.; Xiong, Y. J.; Yoon, J.; Nuzzo, R. G.; Rogers, J. A.; Lewis, J. A. *Science* **2009**, *323*, 1590−1593.
(14) Therriault, D.; White, S. R.; Lewis, J. A. *Nat. Mater.* **2003**, *2*, 265−271.
(15) Kitson, P. J.; Rosnes, M. H.; Sans, V.; Dragone, V.; Cronin, L. *Lab Chip* **2012**, *12*, 3267−3271.

(16) Ilievski, F.; Mazzeo, A. D.; Shepherd, R. E.; Chen, X.; Whitesides, G. M. *Angew. Chem., Int. Ed.* **2011**, *50*, 1890−1895.
(17) Sachs, E.; Cima, M.; Williams, P.; Brancazio, D.; Cornie, J. *J. Eng. Ind-T ASME* **1992**, *114*, 481−488.
(18) Sun, W.; Starly, B.; Nam, J.; Darling, A. *Comput. Aided Des.* **2005**, *37*, 1097−1114.
(19) Genes, L. I.; Tolan, N. V.; Hulvey, M. K.; Martin, R. S.; Spence, D. M. *Lab Chip* **2007**, *7*, 1256−1259.
(20) Toepke, M. W.; Beebe, D. J. *Lab Chip* **2006**, *6*, 1484−1486.